

# Quartz solubility in salt-bearing solutions at pressures to 1 GPa and temperatures to 900°C

Katy Evans<sup>1,2</sup>

<sup>1</sup>RSES, ANU, ACT 0200, Australia

<sup>2</sup>School of Earth Sciences, University of Melbourne, Victoria 3010, Australia

This is the peer reviewed version of the following article:

Evans, K. 2007. Silica solubility in salt-bearing solutions at rpressure to 1 GPa and temperature to 900oC. *Geofluids*. 7 (4): pp. 451-467,

which has been published in final form at <http://doi.org/10.1111/j.1468-8123.2007.00199.x>.

This article may be used for non-commercial purposes in accordance with Wiley Terms and Conditions for Self-Archiving at <http://olabout.wiley.com/WileyCDA/Section/id-828039.html>

## Abstract

An expression that describes the solubility of quartz in alkali-chloride-bearing solutions is derived and applied to literature data on quartz solubility. The model is based on a physically realistic conceptual model that involves salt dissociation as a function of pressure, temperature, and salt concentration, and the presence of hydrated monomer, dimers, and hydrated alkali-silica species. A simplified version of the model that neglects dimerisation and water in the alkali-silica species provides excellent fits to the experimental data with two calibration parameters at each pressure and temperature. The calibration parameters represent the relative stabilities of the alkali-silica and hydrated-silica solute complexes, and the degree of salt dissociation. The success of the model provides support for the existence of an alkali-silica species in salt solutions at low fluid densities.

The model can be interpolated successfully for NaCl-bearing solutions between 0.1 and 1 GPa and from 400 to 900°C, with standard deviations of the predicted from the experimental data of less than 10 percent relative for most conditions. Quartz solubility within this range is described by

$$\frac{X(\text{SiO}_2)}{X(\text{SiO}_{2,\text{ref}})} = \left( \frac{X(\text{H}_2\text{O}_{\text{app}})}{1 + \alpha X(\text{NaCl}_{\text{app}})} \right)^3 + c \left( \frac{\alpha X(\text{NaCl}_{\text{app}})}{1 + \alpha X(\text{NaCl}_{\text{app}})} \right)$$

$X_{i,\text{app}}$  refers to the apparent mole fraction of  $i$ , which is the mole fraction calculated if NaCl is assumed to be totally associated, and  $X(\text{SiO}_{2,\text{ref}})$  is the mole fraction of  $\text{SiO}_2$  in the salt-free solution.

$$c = 37.17 - 0.00141T - 24.45\rho,$$

$$\alpha = 1 - \text{Erf}[dX_{\text{NaCl,app}}],$$

where  $d$  is a calibration parameter that depends on pressure and density as shown below.

$$d = 2.75 - 2.733P + 2.38\rho.$$

$T$  is temperature in Kelvin,  $P$  is pressure in GPa, and  $\rho$  is the density in  $\text{g cm}^{-3}$ . Extrapolation of the expression beyond the calibration range is not recommended. Quartz solubility is additive for mixtures, so silica concentrations in solutions more complex than those covered by the literature data can also be predicted. Fits to the data also enabled regression of thermodynamic data for the proposed  $\text{SiO}_2\cdot(\text{NaCl})_{0.5}$  species.  $H_{298}$  is  $-1040.2 \pm 7.6 \text{ kJ mol}^{-1}$ ,  $S_{298}$  is  $0.169 \pm 0.01 \text{ kJ mol}^{-1} \text{ K}^{-1}$ , and  $V_{298}$  is  $31 \pm 4 \text{ kJ GPa}^{-1} \text{ mol}^{-1}$ .

The model is semi-empirical because the fit parameters are correlated with one of the set parameters, and the use of a simplified mathematical description of salt dissociation. Nevertheless, the model provides an improved method for the calculation of quartz solubility in geological solutions.

## Introduction

Dissolved silica is ubiquitous in crustal fluids, and fluid infiltration followed by quartz dissolution-precipitation reactions alters the rheology (e.g., Lund *et al.* 2006), porosity-permeability structure (e.g. Renard *et al.* 2000; Wark & Watson 2002), and composition (e.g. Bebout & Barton 1993) of crustal rocks. An understanding of processes that control quartz solubility and quantitative description of those processes is, therefore, necessary if regional metamorphism, oceanic hydrothermal systems, subduction complexes and hydrothermal ore-forming environments are to be understood. The solubility of quartz in pure water is well known (Kennedy 1950; Anderson & Burnham 1965, 1967; Crerar & Anderson 1971; Hemley *et al.* 1980; Walther & Orville 1983; Manning 1994) at pressures and temperatures of geological interest. However, natural fluids are compositionally complex, and fluid constituents such as NaCl and CO<sub>2</sub> have a significant, but poorly understood, influence on quartz solubility (e.g. Shmulovich *et al.* 2001; Newton & Manning 2000; Shmulovich *et al.* 2006).

The effects of solutes such as NaCl and CO<sub>2</sub> on quartz solubility vary as a function of pressure, temperature and the identity of the solute. Inert solutes such as CO<sub>2</sub> and argon have been shown to cause significant reductions in quartz solubility with increasing solute concentration at all the pressures and temperatures that have been investigated so far (Sommerfeld 1967; Novgorodov 1975; Walther & Orville 1983; Newton & Manning 2000; Shmulovich *et al.* 2001). All the salts that have been examined also show this type of behaviour, which is also known as salting-out, at high fluid densities (e.g., Newton & Manning, 2000; Shmulovich *et al.* 2001; Shmulovich *et al.* 2006). This type of behaviour is described here as type 1. However, at low fluid densities an initial increase in silica concentration with increasing solute concentration (salting-in), can be followed by a reduction in silica concentration once some critical concentration of the solute is reached (e.g. Fournier & Potter 1982; Xie & Walther 1993; Shmulovich *et al.* 2006). This effect is enhanced for salts that contain large ions such as CsCl (Shmulovich *et al.* 2006). This type of behaviour is described here as type 2. The

two types of behaviour are illustrated in Fig. 1 .

An understanding of the causes of the two types of behaviour is necessary if quartz solubilities are to be predicted at pressures, temperatures, and fluid compositions other than those used for the experiments. Previous workers have shown that type 1 behaviour is consistent with the presence of dissolved silica as a hydrated species of the formula  $\text{SiO}_2 \cdot n\text{H}_2\text{O}$ , where  $n$  is between 2 and 4, and increases with solution density (Sommerfeld 1967; Novgorodov 1975; Walther & Orville 1983; Newton & Manning 2000; Shmulovich *et al.* 2001; Shmulovich *et al.* 2006). The cause of type 2 behaviour (salt-in followed by salt-out) is less clear. Proposed causes for this behaviour include the existence of alkali-silica complexes such as  $\text{H}_3\text{NaSiO}_4$  (e.g. Anderson & Burnham 1983), and changes in the dielectric properties of the solution with increasing salt concentration (e.g. Xie & Walther 1993). Shmulovich *et al.* (2006) obtained a comprehensive dataset in which type 2 behaviour was well represented, but were unable to ascribe type 2 behaviour unambiguously to any particular cause. Instead, they developed an empirical formulation to describe changes in quartz solubility as a function of salt concentration. The formulation describes quartz solubility at the experimental pressures and temperatures well, but it has no physical meaning, so it is difficult to extrapolate or interpolate.

A better understanding of quartz solubility requires more detailed knowledge of the stoichiometry of dissolved silica species. Some spectroscopic information is available at high pressures and temperatures; Raman spectra and solubility data have been used to suggest that dissolved silica begins to form dimers or more complex species at temperatures and pressures greater than 600°C and 0.8 GPa (Zotov & Keppler 2000; Zotov & Keppler 2002; Newton & Manning 2002; Newton & Manning 2003; Newton & Manning 2006). Quartz solubility in solutions with different fixed silica activities at 1.2 GPa and 800°C were modelled successfully as a mixture of coexisting silica monomers and dimers (Newton & Manning 2003; Gerya *et al.* 2005). However, there is little evidence for the identity of the dissolved silica species under the conditions that produce the type 2 (salt-in followed by salt-out) behaviour. Investigations are complicated by variable dissociation of salts in the pressure-

temperature range where type 2 behaviour occurs (Aranovich & Newton 1996; Aranovich & Newton 1997). When salts dissociate the mole fractions of all the species in solution become functions of the degree of dissociation and when the degree of dissociation is unknown, the mole fractions are poorly defined. Further difficulties with identification of silica species result from the use of molal concentration scales by some studies (e.g. Anderson & Burnham 1967; Fournier *et al.* 1982). This is inappropriate for concentrated or mixed solvent solutions because molality and molality-based activities become non-linear functions of solute concentration as the mole fraction of water decreases. These factors result in poorly known salt activities and non-unique solutions for relationships between salt concentration and quartz solubility. Previous attempts to deal with these issues have made a-priori assumptions of the salt speciation and silica species stoichiometry, and dealt with discrepancies between the model and data via ad-hoc non-ideal activity terms (e.g. Anderson & Burnham 1983; Shumlovich *et al.*, 2006). Such approaches are effective but do not further knowledge of the processes that occur in solution.

This study takes a different approach. Expressions based on those that describe ideal mixing are constructed for quartz solubility, where the stoichiometry of the dissolved silica species and the degree of salt dissociation are the unknown parameters. The unknown parameters are calibrated by fitting the expressions to quartz solubility data from the literature. The benefit of this analysis is that the calibrated parameters have physical meaning, which enables more confident interpolation and extrapolation of the expressions, and an increased understanding of the stoichiometry of dissolved silica species.

## **Thermodynamic Background and Methods**

### **Terminology**

The terminology used here is that of Evans & Powell (2006). Briefly, the chemical components of the system are the smallest set of chemical formulae required to describe the

composition of all the phases in the system (c.f. Anderson & Crerar 1993; Nordstrom & Munoz 1994). A species is a molecular or ionic entity which has existence as an identifiable unit (Anderson & Crerar 1993; Nordstrom & Munoz 1994). An end-member is a chemical entity of fixed composition that may be observable or hypothetical, and which may, but need not be, a species (e.g. Thompson 1982). An independent set of end-members is a set of end-members such that it is impossible to create any end-member in the set by linear combination of the other end-members in the set. Relationships between independent end-members are described by an independent set of reactions. The number of independent reactions is the difference between the number of end-members and the number of components. Proportion ( $p$ ), describes the relative quantity of an end-member in an independent set of end-members, where  $p_i = \frac{n_i}{\sum_j n_j}$ ;  $n_i$  is the number of moles of  $i$ , and  $\sum p_i = 1$ . Mole fraction is used to describe the abundance of species.

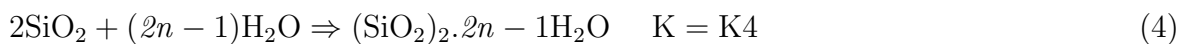
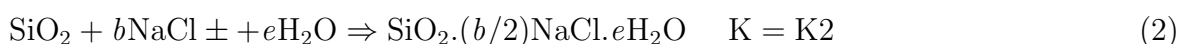
Dissociated salts are represented by a single end-member, identified by a  $\pm$  suffix, as the quantities of anions and cations are not independent because of the charge balance constraint. This representation for dissociated salts is similar to the use of mean ionic compounds (e.g., Nordstrom & Munoz 1994). The stoichiometry of the mean end members is specified to be such that dissolution of one mole of the mean end-member creates one mole of ions in solution. Thus one mole of  $\text{NaCl}\pm$  consists of half a mole each of Na and Cl, and one mole of  $\text{CaCl}_2\pm$  contains one third of a mole of Ca and two thirds of a mole of Cl. This approach simplifies the thermodynamic description of the dissociated salts.

The standard state of end-members for which data is derived from measurements of the pure substance, such as  $\text{H}_2\text{O}$ , is that of unit activity of the pure end-member at the pressure and temperature of interest. The standard state of solute end-members, where thermodynamic data is derived from measurement of the properties of dilute solutions (e.g.  $\text{NaCl}\pm$ ) is a pure hypothetical standard state where  $a_i \rightarrow 1$  as  $x_i \rightarrow 1$  (Raoult's Law) at any pressure and temperature. This standard state has a unit mole fraction of the solute species concerned, but otherwise, the properties are those of the solute in infinitely dilute solution (Stokes 1991), so the standard state is hypothetical. Relationships between standard state

chemical potentials for the mole fraction and molal concentration scales are discussed and illustrated in Evans & Powell (2006) and Stokes (1991).

## Thermodynamic Analysis of the System

The description below uses NaCl as an example, but it can be applied as written to any 1:1 salt, such as KCl or CsCl. It can also be applied, as written, to 1:2 salts or 1:3 salts that partially dissociate (e.g.  $\text{CaCl}_2 \rightarrow \text{CaCl}^+ + \text{Cl}^-$ ), or with adjustments to the stoichiometry, to fully dissociated salts that are not 1:1. The system of interest comprises three components NaCl,  $\text{H}_2\text{O}$  and  $\text{SiO}_2$ . The independent end-members are  $\text{H}_2\text{O}^o(\text{l})$ ,  $\text{NaCl}^o(\text{aq})$ ,  $\text{NaCl}\pm(\text{aq})$  and  $\text{SiO}_2(\text{s})$ , plus end-members to represent dissolved silica. There are an infinite number of possibilities for the dissolved silica end-members, but it is necessary to constrain the stoichiometry to some extent or the system becomes computationally intractable. Initially, silica monomers ( $\text{SiO}_2.n\text{H}_2\text{O}$ ), silica dimers  $(\text{SiO}_2)_2.(2n-1)\text{H}_2\text{O}$ , and an alkali-silica species with or without added water molecules ( $\text{SiO}_2.b\text{NaCl}.e\text{H}_2\text{O}$ ) was considered. There are thus seven independent endmembers, so four independent reactions Eqn (1) to Eqn (4), describe the system:



Note the stoichiometric coefficient for NaCl in the salt-bearing silica species is  $b/2$ , as each molecule of  $\text{NaCl}\pm$  consists of half a molecule each of  $\text{Na}^+$  and  $\text{Cl}^-$ . The same argument determines the stoichiometry of Eqn (3). Dissociation of NaCl is described with the parameter  $\alpha$ , where

$$\alpha = \frac{0.5n_{\text{NaCl}\pm}}{n_{\text{NaCl}_{\text{app}}}}. \quad (5)$$



$\alpha$  is 1 when the solution is completely dissociated and 0 when it is completely associated.

The proportions of  $\text{H}_2\text{O}$ ,  $\text{NaCl}$  and  $\text{NaCl}\pm$  can then be specified in terms of the apparent mole fractions and  $\alpha$  by Eqns (6) to (8), so long as the proportion of dissolved silica species can be neglected. Silica mole fraction is rarely above 0.02, and never higher than 0.045 in the data set we consider here, so this assumption is justified.

$$p(\text{H}_2\text{O}^o) = \frac{1 - X(\text{NaCl}_{\text{app}})}{1 + \alpha X(\text{NaCl}_{\text{app}})} \quad (6)$$

$$p(\text{NaCl}^o) = \frac{(1 - \alpha)X(\text{NaCl}_{\text{app}})}{1 + \alpha X(\text{NaCl}_{\text{app}})} \quad (7)$$

$$p(\text{NaCl}\pm) = \frac{2\alpha X(\text{NaCl}_{\text{app}})}{1 + \alpha X(\text{NaCl}_{\text{app}})} \quad (8)$$

The ideal activities of the uncharged species,  $\text{H}_2\text{O}^o$  and  $\text{NaCl}^o$ , are equal to their proportions. The ideal activity of  $\text{NaCl}\pm$  is different to its proportion because this end-member is not a real species in solution. Activities for mean ionic end-members are discussed by Nordstrom & Munoz (1994) and Evans & Powell (2006). The ideal activity for  $\text{NaCl}\pm$  is

$$a(\text{NaCl}\pm) = \frac{\alpha X(\text{NaCl}_{\text{app}})}{1 + \alpha X(\text{NaCl}_{\text{app}})} \quad (9)$$

The total concentration of dissolved silica is the sum of the hydrous and alkali species:

$$X(\text{SiO}_2,_{\text{tot}}) = \frac{a_{\text{SiO}_2.n\text{H}_2\text{O}}}{\gamma_{\text{SiO}_2.n\text{H}_2\text{O}}} + \frac{a_{\text{SiO}_2.b/2\text{NaCl}.e\text{H}_2\text{O}}}{\gamma_{\text{SiO}_2.b/2\text{NaCl}.e\text{H}_2\text{O}}} + 2 \frac{a_{(\text{SiO}_2)_2.(2n-1)\text{H}_2\text{O}}}{\gamma_{(\text{SiO}_2)_2.(2n-1)\text{H}_2\text{O}}}. \quad (10)$$

If mixing is assumed to be ideal (all  $\gamma$ s are 1), and the solutions are assumed to be in equilibrium with pure quartz with an activity of 1, then Eqns (1), (2), (4) and (10) can be combined and rearranged to give

$$X(\text{SiO}_2,_{\text{tot}}) = K1a(\text{H}_2\text{O}^o)^n + K2a(\text{NaCl}\pm)^b a(\text{H}_2\text{O})^e + 2K4a(\text{H}_2\text{O}^o)^{(2n-1)} \quad (11)$$

The assumption of ideal mixing for the water-NaCl mixture is a simplification. Studies of this, and other salt-bearing systems (e.g. Koster van Groos 1991; Aranovich & Newton 1996; Shmulovich & Graham 1996; Aranovich & Newton 1997) have demonstrated that the

systems are not ideal. However, the majority of activity-composition models that have been developed for the system are unsuitable because salt dissociation, which is a critical feature of this model, is not considered explicitly (e.g. Pitzer 1973; Pitzer 1974). The model of Aranovich & Newton (1996) does consider dissociation, but does not allow it to vary with concentration; this assumption is valid for the concentration range that they considered but is incompatible with the system considered here. The DH-ASF model (Evans & Powell 2006) would be suitable for use in these systems but is not utilised here because this model has been calibrated to compensate for poor conceptual models. Therefore the ideal system is used as far as possible, with non-ideality incorporated only as necessary. Both sides can then be divided by  $X(\text{SiO}_{2,\text{ref}})$ , the solubility of quartz in pure water, which is equal to  $K1+2K4$ , to give

$$\begin{aligned} \frac{X(\text{SiO}_{2,\text{tot}})}{X(\text{SiO}_{2,\text{ref}})} &= \frac{K1}{K1 + 2K4} a(\text{H}_2\text{O}^o)^n + \frac{2K4}{K1 + 2K4} a(\text{H}_2\text{O}^o)^{(2n-1)} + \\ &+ \frac{K2}{K1 + 2K4} a(\text{NaCl}\pm)^b a(\text{H}_2\text{O})^e. \end{aligned} \quad (12)$$

This representation of the contribution of silica dimers to the total silica mole fraction is incorrect, as the number of moles of silica and the silica mole fraction cease to be equivalent once dimers are included. However, the effect of this assumption the results is negligible.  $a(\text{H}_2\text{O}^o)$  and  $a(\text{NaCl}\pm)$  are functions of the known apparent mole fractions and the extent of dissociation, as shown above, so

$$\begin{aligned} \frac{X(\text{SiO}_{2,\text{tot}})}{X(\text{SiO}_{2,\text{ref}})} &= f \left( \frac{1 - X(\text{NaCl}_{\text{app}})}{1 + \alpha X(\text{NaCl}_{\text{app}})} \right)^n + (1 - f) \left( \frac{1 - X(\text{NaCl}_{\text{app}})}{1 + \alpha X(\text{NaCl}_{\text{app}})} \right)^{(2n-1)} \\ &+ c \left( \frac{\alpha X(\text{NaCl}_{\text{app}})}{1 + \alpha X(\text{NaCl}_{\text{app}})} \right)^b \cdot \left( \frac{1 - X(\text{NaCl}_{\text{app}})}{1 + \alpha X(\text{NaCl}_{\text{app}})} \right)^e \end{aligned} \quad (13)$$

Where  $c$  is equal to  $\frac{K2}{K1+2K4}$  and  $f$  is  $\frac{K1}{K1+2K4}$ . Eqn (13) expresses the concentration of dissolved silica in equilibrium with quartz as a function of the apparent salt concentration and six adjustable parameters:  $n$ , the number of waters of hydration on the hydrated quartz monomer;  $b$ , the number of moles of NaCl complexed with silica;  $c$ , which represents the

relative stability of the alkali and combined hydrous species;  $e$ , the number of moles of  $\text{H}_2\text{O}$  complexed with the alkali-silica species;  $f$ , which represents the relative stability of the silica monomer and dimer species, and  $\alpha$ , the extent of dissociation.  $\alpha$  is a function of the salt concentration (e.g. Sherman & Collings 2002) and can be expressed in terms of  $K3$  and  $X(\text{NaCl}_{\text{app}})$  (Eqn (14)).

$$\alpha_K = \frac{-K3 + K3X_{\text{NaCl,app}} + \sqrt{K3} \sqrt{K3 + 4X_{\text{NaCl,app}} + 2K3X_{\text{NaCl,app}} + K3X_{\text{NaCl,app}}^2}}{2(X_{\text{NaCl,app}} + K3X_{\text{NaCl,app}})} \quad (14)$$

where  $\alpha_K$  denotes  $\alpha$  values derived from the  $K$ -based expression.  $\alpha_K$  values derived from Eqn (14) and the thermodynamic data of Holland & Powell (1998) did not form the basis of good fits to the model. This is attributed mainly to difficulties with extrapolation of data acquired at low temperature to the pressures and temperatures of interest, and also to non-ideal mixing in the systems of interest. A simpler alternative that produced excellent fits to the model is the function defined by Eqn (15), where  $d$  is an adjustable parameter.

$$\alpha_d = 1 - \text{Erf}[dX_{\text{NaCl,app}}]. \quad (15)$$

$\alpha_d$  indicates  $\alpha$  values derived from Eqn (15). Eqn (14) and Eqn (15) produce similar relationships between  $\alpha$  and  $X_{\text{NaCl,app}}$  (Fig. 2). High  $d$  values favour the associated species (low  $\alpha_d$ ), while high  $K3$  values favour the dissociated species (high  $\alpha_K$ ). Eqn (15) is used for the calculation of  $\alpha$  for the remainder of this work, and the  $d$  subscript is dropped from here onwards.

Eqn (13) provides a flexible way to describe the concentration of dissolved silica (Fig. 3). Salting-in and type 2 behaviour are predicted when the alkali-silica species is stable relative to the hydrous species (high  $c$ : Fig. 3A), and when the dissociated salt is favoured (low  $d$ : Fig. 3B). Salting-in occurs at low fluid densities when the salt is mostly associated, so it seems likely that type 2 behaviour is mainly controlled by the relative stabilities of the hydrous and alkali-bearing species. Large values for the numbers of waters of hydration ( $n$ ) reduce salting-in by increasing the dependence of quartz solubility on water activity (Fig. 3C). Salting-in is also optimised by low values for the number of salt molecules associated

with each dissolved silica molecule (low  $b$ : Fig. 3D), as this maximises the number of alkali-silica species that can be formed.

The number of data available at any pressure and temperature is insufficient to constrain six adjustable parameters. However,  $n$  is known from previous studies to vary from 2 to 4 (e.g. Newton & Manning 2000; Shmulovich *et al.* 2006), and preliminary investigations for this study showed that good fits were only obtained when  $b$  was set equal to 1. Further investigation showed that good fits could be obtained for a wide range of  $f$  and  $e$  values; these parameters were highly correlated with the other fit parameters, and exerted only a second order influence on the details of the fit. For convenience, therefore,  $f$  was set to 1, equivalent to neglecting the aqueous silica dimer, and  $e$  was set to 0, which implies that the alkali-silica species was anhydrous. These assumptions are unlikely to be correct; however the data is insufficient to constrain their values, so the set values can be considered to be within model error of the true values. A nonlinear regression routine was then used to obtain  $c$  and  $d$  for each of the datasets considered from the literature. The data included is summarised in Table 1. Good fits were obtained for  $n$  between 2 and 4 for most conditions, but in the interests of consistency  $n$  was set to 3 for NaCl and CsCl. The implications of this decision, and the extent of correlations between  $n$  and the fit parameters, are discussed below.

## Results

The model fits most of the data very well when  $n$ , the number of waters of hydration, is set to 3, and  $b$  the number of salt molecules associated with the alkali-silica species, is set to 1. The standard deviation of the model from the data was, in most cases, less than experimental error. Fit parameters and standard deviations are summarised in Table 2. Fits to the medium to high pressure NaCl data (Fig. 4) give a value for  $c$  that increases as the density of the solution decreases. This is consistent with an alkali-silica species which becomes more stable, relative to the hydrous silica species, as density decreases. The  $d$  parameter, which

determines the extent of salt dissociation, is relatively constant, but decreases with pressure, indicating that dissociation becomes more prevalent at high pressure. This is consistent with interpretations of salt dissociation based on experimental measurements of water activities (Aranovich & Newton 1996; Shmulovich & Graham 1996). Fits to the low pressure NaCl data (Fig. 5A,B) are consistent with this trend. The KCl data of Anderson & Burnham (1967) fit well to the model (Fig. 5C,D). However it is interesting to note the high values of  $c$  and  $d$  that are calculated for the 0.4 GPa data. These indicate that the alkali-silica species is not required for the data to fit the model, so the  $c$  and  $d$  parameters, which are highly correlated (see below), become poorly defined, drift to high values during the non-linear regression, and have large associated uncertainties. Changes in the specified  $n$  parameter can be made to obtain results that are more consistent with those for other datasets in this study, but also result in a loss of integrity for the model.

Fits to the CsCl data (Fig. 6) show similar trends to that for NaCl. However,  $d$  values are lower than for those for NaCl at similar pressures, which indicates a higher degree of dissociation, and the  $c$  value is greater than that for NaCl under similar conditions, which indicates that the CsCl-SiO<sub>2</sub> species is more stable than the equivalent species for NaCl.

The CaCl<sub>2</sub> data fits well to the dataset that shows type 2 behaviour (Figure 7A). However, fits to the other datasets are more problematic. If  $n$  is set to 3 then negative  $c$  values are obtained by the fit.  $c$  is the ratio between two stability constants, both of which are positive, so negative  $c$  values are physically impossible and must flag a problem with the model. Fits to the data were not improved by variation in the set values for  $f$ , which represents the relative stability of monomer and dimer aqueous silica species, or by incorporation of non-zero values for  $e$ , the number of waters associated with the Ca-silica species. The fits shown in Fig. 7B, C, and D, were obtained with a very simple model, in which CaCl<sub>2</sub> was assumed not to dissociate or form an Ca-silica species (i.e.  $c$  and  $d$  were equal to zero). The model was fit for  $n$  with resultant  $n$  values of 4.5 to 9, with  $n$  increasing with increasing solution density. These  $n$  values are higher than those obtained for  $n$  in H<sub>2</sub>O-CO<sub>2</sub> solutions under similar conditions (Newton & Manning 2000). The physical implication of this finding is that

CaCl<sub>2</sub> somehow induces a completely different stoichiometry for the aqueous silica species, which seems unlikely. Possible modifications to the model that might allow a physically reasonable explanation for quartz solubility in CaCl<sub>2</sub>-bearing fluids are discussed below.

## Discussion

### Interpolation and extrapolation of the model

A way to test the model is to assess the degree to which it can be interpolated and extrapolated. For this, a subset of the NaCl data was used to parameterise the fit parameters  $c$  and  $d$ . The datasets used are marked with an asterisk in Table 2. The four variables investigated for the parameterisation were pressure, temperature, density, and dielectric constant. Density is itself a function of pressure and temperature, but its inclusion in the list is useful, as thermodynamic properties of aqueous species in solution have been shown to correlate more closely with density than with either pressure or temperature alone (e.g. Anderson *et al.* 1991). The dielectric constant is included because it measures the degree of hydrogen bonding in solution, and thus the ability of water to hydrate ions, which favours dissociated over associated salts. Dielectric constants were calculated with the Archer & Wang (1990) formulation for the dielectric constant of pure water. The effect of salt on dielectric constant was not included, although this would have some effect. Density was calculated using the CORK (Compensated Redlich-Kwong) model (Holland & Powell 1991). A variety of functional relationships were tried against the fit  $c$  and  $d$  values. These included linear, power law, logarithmic and polynomial functions. The ability of the different relationships to replicate the fit parameters was measured via the standard deviation between the predicted and calibrated parameters for the chosen conditions. The more complex relationships did not offer any significant advantage over the simpler relationships, so the chosen empirical functions were of the form  $u + v p1 + w p2$ , where  $u$ ,  $v$  and  $w$  are constants and  $p1$  and  $p2$  are the chosen parameters. All the possible combinations of two out of the four parameters

were tried against this relationship (Table 3). Results showed that density and temperature offered the best predictors for  $c$  while density and pressure provided the best fit for  $d$ . The agreement between the predicted and fit parameters is reasonable (Fig. 8A, 8B), although the data is scattered about the 1:1 line. This fit was deemed acceptable given the sparsity of the data. Quartz solubility can, therefore be calculated from Eqns (13) and (15), with  $n$ ,  $b$ ,  $e$  and  $f$  set to 3, 1, 0, and 1 respectively,  $c$  given by

$$c = 37.17 - 0.00141T - 24.45\rho, \quad (16)$$

and  $d$  by

$$d = 2.75 - 2.733P + 2.38\rho. \quad (17)$$

Solubility is as a fraction of the mole fraction of silica in pure water,  $T$  is temperature in Kelvin,  $P$  is pressure in GPa, and  $\rho$  is the density in  $\text{g cm}^{-3}$ . The difference in the best predictor parameters for  $c$  and  $d$  is interesting; the occurrence of temperature as a predictor for  $c$  implies that the value of  $c$  is controlled by the entropy change associated with the formation of the two species. The occurrence of pressure as a predictor for  $d$  indicates that the change in volume associated with ion association has a strong effect on the thermodynamics of this equilibrium. The relationship between both parameters and density is likely to record the effect of average distances between salt and silica molecules on the probability of complex formation and ion association. The weak relationship between dielectric constant and  $c$  and  $d$  is noteworthy, as dielectric effects have been invoked as the cause of the change between salting-in and salting-out (Xie & Walther 1993). The lack of a relationship here implies that either the dielectric effects are insufficient to cause such changes, or that the lack of inclusion of salt contributions to the calculated dielectric constant masks any such changes.

The predictive quality of the model was then tested with calculations of fits of the model to the data using predicted parameters for all datasets, including those not used in the initial fit (Figs. 8C,D). Standard deviations to these fits ( $\sigma_{\text{ex}}$ ; Table 2) indicate that the fit is good, with standard deviations of less than 10 percent relative in silica concentrations for

most pressures and temperatures within the calibrated range. The fit was worse with a 20 percent relative standard deviation in quartz solubility for the highest pressure dataset (1.5 GPa), which was included in the fitting algorithm. One explanation is that the presence of silica dimers increases significantly for this dataset (Newton & Manning 2003; Gerya *et al.* 2005; Newton & Manning 2006). Explicit incorporation of dimers is possible with the model used here, but the lack of intermediate data between 1GPa and 1.5GPa prevents effective calibration of dimerisation-related parameters. Attempts at fitting without the 1.5 GPa dataset did not improve results for the medium pressure data, and worsened that for the 1.5 GPa data, so its inclusion was retained. Extrapolation to the lowest pressures (0.02 to 0.05 GPa) was unsuccessful, with standard deviations of around 30 percent in relative quartz solubility (Table 2). Fitting of the calibration parameters for the CsCl and KCl was not performed, as the number of data was insufficient for this procedure. Overall, the interpolative ability of the algorithm derived here was judged to be adequate, as the change from type 1 to type 2 behaviour was predicted successfully.

### Correlation of fit parameters

The degree of correlation between  $n$  which was set for the fitting, with the fit parameters  $c$  and  $d$  was also investigated using the 1 GPa, 800°C data from Newton & Manning (2000). Fits to the model were made using values of  $n$  between 2 and 6, and the relationships between  $n$ ,  $c$ ,  $d$  and the goodness of fit were assessed (Fig. 9). The fits were good for the whole range of  $n$  values tried, with standard deviations between 1 and 3 percent relative quartz solubility (Fig. 9A).  $n$  and  $c$  were positively correlated (Fig. 9B), whereas the relationship between  $n$  and  $d$  was more complex (Fig. 9C), with a maximum in  $d$  for  $n$  around 3.3, and an accompanying minimum in the standard deviation (Fig. 9D). This maximum indicates the point where the solution to the model equation becomes poorly defined as a result of the alkali-silica species becoming superfluous, as discussed above for the AB67 KCl data. Maxima such as these are not seen for type 2 datasets where the alkali-silica species is necessary to produce the salt-in-salt-out behaviour. The maximum also causes the maximum in the  $c$  versus  $d$  plot



(Fig. 9D). Good model fits were not obtained for  $b$  values different to 1, so exploration of correlation between this parameter and  $c$  and  $d$  was not necessary.

To summarise, the calculated solutions are non-unique and correlations between the calibrated parameters show non-linear behaviour.  $n$  is therefore poorly constrained, and further experimental investigation is necessary to measure the stoichiometry of the hydrous silica species. However, the model still allows successful prediction of quartz solubility (see above) and an increased understanding of the physical processes that occur in solution.

### Application to mixed salt solutions

The form of Eqn (13) facilitates its expansion and application to mixed salt solutions. If it is assumed that the thermodynamics of mixed salt solutions can be described by Eqn (1) and a pair of equations of the form of Eqns (2) and (3) for each salt in the solution, then the quartz solubility is

$$\frac{X(\text{SiO}_{2,\text{tot}})}{X(\text{SiO}_{2,\text{ref}})} = \left( \frac{X(\text{H}_2\text{O}_{\text{app}})}{1 + \sum_j \alpha_j X(\text{j}_{\text{app}})} \right)^3 + \sum_j c_j \left( \frac{\alpha_j X(\text{j}_{\text{app}})}{1 + \sum_j \alpha_j X(\text{j}_{\text{app}})} \right) \quad (18)$$

where the sum is over  $j$ , the number of different salts in solutions. Each of the  $c_j$  and  $\alpha_j$  need to have been determined from experiments on single salt solutions. Eqn (18) is valid if there are no mixed salt-silica species, and if the extent of salt dissociation is not affected by the presence of multiple salts. The latter condition may fail in concentrated solutions, but further experimental work is required to verify this.

### The use of Erf in the dissociation term

The use of an error function in Eqn(15) as part of the definition of  $\alpha$ , which measures dissociation, is an approximation that was introduced to make the system more tractable, and retained because it produced good results. It produces a similar functional relationship between  $\alpha$  and  $X_{\text{NaCl,app}}$  to Eqn (14). Dissociation calculated using Eqns (14) and 15) was

compared with that calculated with THERMOCALC (Holland & Powell, 1998; Powell *et al.* 1998) for the NaCl-H<sub>2</sub>O system at 0.8 GPa and 500°C (Fig. 10). THERMOCALC calculations used the DH-ASF activity-composition model described by Evans & Powell (2006), and activity coefficient parameters calibrated by fitting to data from Aranovich & Newton (1996) and Koster van Groos (1991). The three estimates agree at low apparent salt concentrations but diverge with increasing salinity. Dissociation calculated with the Erf-based model lies between the strict ideal model and the DH-ASF activity composition model. Thus, the use of the Erf approximation introduces a degree of empiricism to the model that compensates for the use of ideal activity-composition relationships. However the precise reason for its success is unclear.

### **Physical representation of CaCl<sub>2</sub>-H<sub>2</sub>O-SiO<sub>2</sub>**

The assumption that speciation in CaCl<sub>2</sub>-H<sub>2</sub>O-SiO<sub>2</sub> can be represented by an associated salt species, CaCl<sub>2</sub><sup>°</sup>, a single charged salt species, CaClCl<sup>±</sup>, water, a hydrous silica monomer, SiO<sub>2</sub>.*n*H<sub>2</sub>O, a calcium-bearing silica species with or without water, SiO<sub>2</sub>.*e*H<sub>2</sub>O.*c*CaClCl<sup>±</sup>, and a hydrous silica dimer (SiO<sub>2</sub>)<sub>2</sub>.*2n-1*.H<sub>2</sub>O, does not form the basis of a successful conceptual model for quartz solubility in this system, regardless of the value of parameters chosen to describe the stoichiometry of the species and the relative stability of the different silica species. This is in marked contrast to the success of the conceptual model when applied to alkali chloride-bearing systems.

Inspection of a comparison of the quartz solubility data for different solutes reveals that a major difference between the alkali chloride and Ca-bearing systems is that the alkali chlorides induce salting-in relative to CO<sub>2</sub>-bearing solutions, whereas, at fluid densities greater than 0.7 g cm<sup>-3</sup>, Ca causes salting-out, relative to CO<sub>2</sub>-bearing solutions (Fig. 11A). This observation explains the failure of the conceptual model to describe the system, as the salt-silica species can only mimic salting-in relative to the CO<sub>2</sub>-bearing system. The additional salting-out is consistent with a decrease in water activity in the CaCl<sub>2</sub>-bearing system that

is greater than the decrease in water activity caused by  $\text{CO}_2$ . Reduced water activity destabilises the hydrous silica species, and results in a reduced quartz solubility, as observed.

Full dissociation of  $\text{CaCl}_2$  would cause such a decrease in water activity; the presence of a larger number moles of the dissociated salt would reduce the water mole fraction, and hence its activity. This is demonstrated in Fig. 11B, which compares the predicted solubility of quartz as  $\text{SiO}_2 \cdot 3\text{H}_2\text{O}$  in solutions that contain fully, partially, and totally dissociated  $\text{CaCl}_2$ , with the observed data at 0.5 GPa and  $800^\circ\text{C}$ . The data falls between the predicted lines for partially and totally dissociated  $\text{CaCl}_2$ . The problem with this explanation is that it seems unlikely that  $\text{CaCl}_2$  is significantly dissociated at these pressures and temperatures. Calcium has a large charge:radius ratio, which enhances ion association, and so  $\text{CaCl}_2$  would be expected to be more associated than the alkali chlorides under these conditions. This is consistent with the results of Fulton *et al.*, (2006), who note that ion association is significant in solutions with a density of  $0.64 \text{ g cm}^{-3}$  at  $400^\circ\text{C}$  at pressures to 0.035 GPa, but experimental constraints at the higher pressures, temperatures and fluid densities that are relevant to this study are lacking.

Dimerisation or hydration of the aqueous species in the  $\text{CaCl}_2$ -bearing solutions in excess of that that would occur in a  $\text{CO}_2$ -bearing solution of equivalent concentration would also cause excess salting-out behaviour. However, it seems unlikely that species that do not incorporate Ca or Cl would behave differently simply because of the presence of a salt, although such a phenomenon has been proposed to be a consequence of salt-induced changes in the electrical properties of the solution (Newton & Manning 2006).

An alternative possibility is that waters that are solvated to Ca or Cl in solution are unavailable for the formation of aqueous silica species, with a consequent reduction in the water activity. Waters of solvation were not included in the model for the alkali chlorides because the data fit well without this additional complication. The implication of this result is that waters solvated to alkali chlorides are available for quartz dissolution, and/or that waters of solvation become involved in the formation of silica complexes; this latter option would be consistent with hydrous alkali-silica complexes. However, the larger size and more

complex geometry of the Ca-bearing complexes in solution may provide an effective barrier to the participation of solvated waters in silica dissolution. If this is the case then water activity is reduced by ion solvation, with a consequent reduction in the stability of aqueous silica complexes and quartz solubility. This hypothesis was explored by the calculation of theoretical solubility curves for a variety of solvation scenarios that involved only an aqueous silica monomer (Fig. 11C). A new parameter,  $g$ , was introduced to represent the number of solvated waters on the salt species and it was found that the best results were obtained when it was considered that only the charged species became solvated. Under these circumstances the ratio of quartz solubility to that in pure water is given by

$$\frac{X(\text{SiO}_{2,\text{tot}})}{X(\text{SiO}_{2,\text{ref}})} = a(\text{H}_2\text{O}^o)^n \quad (19)$$

where

$$a(\text{H}_2\text{O}^o) = \frac{1 - X(\text{CaCl}_2, \text{app}) - gX(\text{CaCl}_2, \text{app})(1 + \alpha)}{1 - gX(\text{CaCl}_2, \text{app})(1 + \alpha) + \alpha X(\text{CaCl}_2, \text{app})} \quad (20)$$

It was found that the additional salting-out observed in the data could be accounted for by a combination of moderate salt dissociation ( $d=2$ ) and one or two solvated waters on each dissociated salt molecule ( $g=1$  or  $g=2$ ), with the greater solvation predicted at higher fluid densities, which is consistent with physical expectations. However, there is no experimental or theoretical evidence to either support or refute this hypothesis.

### Extraction of thermodynamic data and use for prediction

Thermodynamic data for the NaCl-silica species was determined from the literature data and the calibrated model parameters. Literature data is taken from Holland & Powell (1998). The equation of state (EOS) for aqueous species is that of Anderson *et al.* (1991), modified according to Holland & Powell (1998), and adjusted to give a standard state with a mole fraction of unity (Evans & Powell 2006).

$K1$  (Eqn (1)) for each NaCl-bearing dataset was calculated using thermodynamic data from the literature.  $K2$ , which is the product of  $K1$  and  $c$ , was then calculated for each

dataset. A value for the Gibbs energy of the aqueous species for each dataset was then calculated from Eqn (21), which is based on Eqn (2).

$$G_{\text{SiO}_2.\text{NaCl}_{0.5}}^{\ominus} = -RT \ln K_2 - G_{\text{SiO}_2(\text{s})}^{\ominus} - b.G_{\text{NaCl}\pm(\text{aq})}^{\ominus} \quad (21)$$

$b$  is set to 1 for all datasets. The estimates of the Gibbs energy for the alkali-silica species were then regressed, using a non-linear regression algorithm, against the equation of state used for the other aqueous species. The EOS requires five input parameters;  $H_{298}$ ,  $S_{298}$ , and  $V_{298}$ , and two heat capacity-related parameters. Regression for the parameters for the alkali-silica species was initially performed with the heat capacity terms set to zero. The results are reasonable and give relatively small uncertainties for  $H_{298}$  and  $S_{298}$  (Eqn (22)), but  $V_{298}$  was poorly defined, see discussion below.

$$\begin{aligned} H_{298} &= -1040.2 \pm 7.6 \text{ kJ mol}^{-1} \\ S_{298} &= 0.169 \pm 0.01 \text{ kJ mol}^{-1} \text{ K}^{-1} \\ V_{298} &= 31 \pm 4 \text{ kJ GPa}^{-1} \text{ mol}^{-1}. \end{aligned} \quad (22)$$

Subsequent regressions that incorporated one or both heat capacity coefficients gave results that were within error of the initial estimates, but the uncertainties on all parameters were much larger for these fits, so the simple estimate is preferred. The standard deviation of the fit from the data was 6.5 kJ, so the fit can be considered successful.

The small number of data points raises questions about the ability of the regression to obtain robust results. For this reason the regression was tested using known values of  $G^{\ominus}$  for NaCl $\pm$  for each of the available pressures and temperatures. Ideally such a regression would reproduce the known values for the NaCl $\pm$  thermodynamic parameters. The parameters obtained from the three parameter regression (Eqn (23)) are within error of the known values, except for the  $V_{298}$ .

$$\begin{aligned} H_{298} &= -188.4 \text{ (203.7)} \pm 7 \text{ kJ mol}^{-1} \\ S_{298} &= 0.0654 \text{ (0.057)} \pm 0.009 \text{ kJ mol}^{-1} \text{ K}^{-1} \\ V_{298} &= -9.08 \text{ (8.34)} \pm 3.5 \text{ kJ GPa}^{-1} \text{ mol}^{-1}. \end{aligned} \quad (23)$$

The figures in brackets are the literature values for the calculated parameters. Discrepancies are attributed to the lack of inclusion of heat capacity parameters, and to the wide range of the data in pressure and temperature space. The large difference between the literature and fit values for  $V_{298}$  is consistent with the lack of a strong pressure effect on the  $c$  parameter, from which the thermodynamic data is derived.

The thermodynamic data derived and presented here are likely to be robust, but are dependent on the model that underlies their derivation. Care should be taken, therefore, if they are to be used with another conceptual model or with thermodynamic data that may be inconsistent with that used here. However, the relatively small uncertainties suggest that the data should be useful so long as it is used in an appropriate context.

### Comparison with recent work

A number of recent studies have explored the relationship between quartz solubility on the concentration on salts in aqueous solution. It is useful to make a qualitative comparison of the results of these studies, though It is not possible to compare derived parameters for the different models because of the different conceptual models that underlie the derivations.

Shmulovich *et al.* (2006) produced an extensive experimental dataset, which was used to calibrate expressions of the form

$$\frac{m_{\text{SiO}_2}}{m_{\text{SiO}_2,\text{ref}}} = X_{\text{H}_2\text{O},\text{app}}^{3.5} + \exp[j \cdot m_{\text{salt},\text{app}}^k] \quad (24)$$

where  $m$  is molality, and  $h$  is a calibration parameter. Eqn (24) is qualitatively similar to that described here; salting out is accounted for by the formation of an aqueous silica monomer with 3.5 waters of hydration, and salting-in is accounted for by a term related to the salt concentration. The exponential part of the expression results in prediction of quartz solubility similar to that predicted with the assumption of an alkali-silica species, although this proposal is not made in the original paper, and the form of the expression is empirical rather than based on consideration of mixing properties in solution.

Studies by Newton & Manning (2002; 2003; 2006) have developed a conceptual model that combines monomer and dimer quartz species with a fused salt solvent model to account for silica concentrations in solutions equilibrated with low silica-activity assemblages (enstatite-forsterite, forsterite-rutile-geikelite, kyanite-corundum-quartz), and NaCl-H<sub>2</sub>O solutions. The model predicts silica concentrations successfully at the experimental conditions, which are in the type 1, salting-out, region of pressure-temperature space, and is consistent with spectroscopic measurements of dimerisation by Zotov & Keppler (2000; 2002). The model does not predict type 2 solubility characteristics or silica concentrations in wollastonite solubility experiments (Newton & Manning 2006), where salting-in behaviour is observed. A hydrous alkali-silica species, H<sub>3</sub>NaSiO<sub>4</sub>, is proposed to account for silica solubility in the latter case, although the stoichiometry of this species is not uniquely constrained by the experimental data.

## Conclusions

Type 1 and Type 2 quartz solubility for NaCl-, KCl- and CsCl-bearing solutions are represented well by a model that includes a hydrated silica monomers, dimers, and an alkali-silica species that may include water. The simplest model to represent the data satisfactorily describes the speciation of silica in aqueous solutions as a combination of SiO<sub>2</sub>.3H<sub>2</sub>O, and SiO<sub>2</sub>.(salt)<sub>0.5</sub>. This model involves two calibrated parameters at each pressure and temperature. The first,  $c$ , represents the relative stabilities of the alkali-silica and hydrated silica species. The second,  $d$ , is a proxy for the changes in salt dissociation as a function in salt concentration. The fit parameters indicate that the alkali-silica species and dissociated salts are more prevalent at low fluid densities, which is consistent with experimental observation. The CsCl-silica species is more stable than the NaCl-silica species. Standard deviations of the model from the experimental data are of the magnitude of experimental uncertainties or smaller for most experiments.

Data for CaCl<sub>2</sub>-bearing solutions are not represented well by the model, mainly because

CaCl<sub>2</sub> causes salting-out to a greater extent than that induced by CO<sub>2</sub>, which cannot be described by the model. This additional salting-out is consistent with water activities in the CaCl<sub>2</sub>-bearing solutions that are lower than has been previously assumed. Possible explanations for this are that the CaCl<sub>2</sub> is extensively dissociated, which is physically unlikely, and/or that waters of hydration on solvated Ca-species are unavailable for salt dissolution and therefore effectively reduce the activity of water. Further experimental evidence is required to test these hypotheses.

Fits at individual temperatures and pressures for NaCl can be interpolated between 0.1 and 1 GPa, and 400 and 900°C.  $c$  is expressed in terms of temperature and solution density, and  $d$  in terms of pressure and solution density. The sensitivity of  $c$  to temperature indicates that the entropic consequences of the formation of the aqueous and alkali-silica species are significantly different.  $d$  is more sensitive to pressure than temperature, which indicates that the volume change involved in salt dissociation has an important effect on the thermodynamics of the dissociation reaction. Both parameters are sensitive to density, which is attributed to the importance of average nearest-neighbour distances for the thermodynamics of solution. Extrapolation of the parameterisation to pressures greater than 1 GPa or less than 0.1 GPa is not recommended.

Regression of the fits to the data gave thermodynamic data for the SiO<sub>2</sub>.(NaCl)<sub>0.5</sub> species.  $H_{298}$  is  $-1040.2 \pm 7.6$  kJ mol<sup>-1</sup>,  $S_{298}$  is  $0.169 \pm 0.01$  kJ mol<sup>-1</sup> K<sup>-1</sup>, and  $V_{298}$  is  $31 \pm 4$  kJ GPa<sup>-1</sup> mol<sup>-1</sup>. The standard deviation of the regressed Gibbs energies from the values calculated from the model fit was 6.5 kJ mol<sup>-1</sup>, which gives confidence in the fit. However, the data is dependent on the assumptions used in its derivation and it may not be compatible with thermodynamic data or activity-composition models other than those used in its derivation.

The model provides a successful interpretation of the experimental data that is based on a physically realistic conceptual model, but the conceptual model is not unique. The fit parameters are correlated with the fixed parameters that specify the stoichiometry of the hydrated silica species. Independent constraints on the stoichiometry of the aqueous silica



species are required to reduce the range of solutions available. The use of a proxy for the degree of dissociation introduces a further degree of empiricism to the model.

To summarise, further experimental and theoretical work is needed to produce a fully process-based model. However, the current semi-empirical model provides excellent fits to existing data, provides insights into the physical processes that accompany silica dissolution, and supports the existence of an alkali-silica species. Interpolation of the fit data allows prediction of quartz solubility in salt solutions over a wide pressure and temperature range.

### Acknowledgements

Thanks for thought-provoking reviews from Craig Manning and Kiril Shmulovich, and to Roger Powell for helpful discussions. KE is supported by Australian Synchrotron Research Program Fellowship and the work was further supported by the Australian Synchrotron Research Program, which is funded by the Commonwealth of Australia under the Major National Research Facilities Program.

### References

- Anderson GM, Burnham CW (1965). Solubility of quartz in supercritical water. *American Journal of Science* **263**, 494-511.
- Anderson GM, Burnham CW (1967). Reactions of quartz and corundum with aqueous chloride and hydroxide solutions at high temperatures and pressures. *American Journal of Science* **265**, 12-27.
- Anderson GM, Burnham CW (1983). Feldspar solubility and the transport of aluminum under metamorphic conditions. *American Journal of Science* **283-A**, 283-297.
- Anderson GM, Castet S, Schott J, Mesmer RE (1991). The density model for estimation of thermodynamic parameters of reactions at high temperatures and pressures.

*Geochimica Et Cosmochimica Acta* **55**, 1769-1779.

Anderson GM, Crerar DA, (1993) Thermodynamics in geochemistry. The equilibrium model. Oxford University Press.

Aranovich LV, Newton RC (1997). H<sub>2</sub>O activity in concentrated KCl and KCl-NaCl solutions at high temperatures and pressures measured using the brucite-periclase method. *Contrib. Mineral. Petrol.* **127**, 261-271.

Aranovich LY, Newton RC (1996). H<sub>2</sub>O activity in concentrated NaCl solutions at high pressures and temperatures measured by the brucite-periclase equilibrium. *Contributions to Mineralogy and Petrology* **125**, 200-212.

Archer DG, Wang PM (1990). The dielectric-constant of water and Debye-Huckel limiting law slopes. *Journal of Physical and Chemical Reference Data* **19**, 371-411.

Bebout GE, Barton MD (1993). Metasomatism during subduction - products and possible paths in the Catalina schist, California. *Chemical Geology* **108**, 61-92.

Crerar DA, Anderson GM (1971). Solubility and solvation reactions of quartz in dilute hydrothermal solutions. *Chemical Geology* **8**, 107-122.

Evans K, Powell R (2006). A method for activity calculations in saline and mixed solvent solutions at elevated temperature and pressure: A framework for geological phase equilibria calculations. *Geochimica et Cosmochimica Acta* **70**, 5488-5506.

Fournier RO, Rosenbauer RJ, Bischoff JL (1982). The solubility of quartz in aqueous sodium-chloride solution at 350-degrees-C and 180 to 500 bars. *Geochimica et Cosmochimica Acta* **46**, 1975-1978.

Fulton JL, Chen YS, Heald SM, Balasubramanian M (2006). Hydration and contact ion pairing of Ca<sup>2+</sup> with Cl<sup>-</sup> in supercritical aqueous solution *Journal of Chemical Physics* **125** 0.94507-1 - 0.94507-10.

- Gerya TV, Maresch WV, Burchard M, Zakhartchouk V, Doltsinis NL, Fockenberg T (2005). Thermodynamic modeling of solubility and speciation of silica in H<sub>2</sub>O-SiO<sub>2</sub> fluid up to 1300 degrees C and 20 kbar based on the chain reaction formalism: *European Journal of Mineralogy* **17**, 269-283.
- Hemley JJ, Montoya JW, Marinenko JW, Luce RW (1980). Equilibria in the system Al<sub>2</sub>O<sub>3</sub>-SiO<sub>2</sub>-H<sub>2</sub>O and some general implications for alteration-mineralization processes. *Economic Geology* **75**, 210-228.
- Holland T, Powell R (1991). A Compensated-Redlich-Kwong (CORK) equation for volumes and fugacities of CO<sub>2</sub> and H<sub>2</sub>O in the range 1-bar to 50-kbar and 100-1600-degrees-C. *Contributions to Mineralogy and Petrology* **109**, 265-273.
- Holland TJB, Powell R (1998). An internally consistent thermodynamic data set for phases of petrological interest. *Journal of Metamorphic Geology* **16**, 309-343.
- Kennedy G (1950). A portion of the system silica-water. *Economic Geology* **45**, 629-653.
- Koster van Groos AF (1991). Differential thermal analysis of the liquidus relations in the system NaCl-H<sub>2</sub>O to 6 kbar. *Geochimica Et Cosmochimica Acta* **55**, 2811-2817.
- Lund MD, Piazzolo S, Harley SL (2006). Ultrahigh temperature deformation microstructures in felsic granulites of the Napier complex, Antarctica. *Tectonophysics* **427**, 133-151.
- Manning CE (1994). The solubility of quartz in H<sub>2</sub>O in the lower crust and upper mantle. *Geochemica et Cosmochimica Acta* **58**, 4831-4839.
- Newton RC, Manning CE (2000). Quartz solubility in H<sub>2</sub>O and H<sub>2</sub>O-CO<sub>2</sub> solutions at deep crust-upper mantle pressures and temperatures: 2-15 kbar and 500-900°C. *Geochemica et Cosmochimica Acta* **64**, 2993-3005.
- Newton, RC, Manning CE (2002). Solubility of enstatite plus forsterite in H<sub>2</sub>O at deep crust/upper mantle conditions: 4 to 15 kbar and 700 to 900 degrees C *Geochimica et Cosmochimica Acta*, **66** 4165-4176.

- Newton RC, Manning CE (2003). Activity coefficient and polymerization of aqueous silica at 800 degrees c, 12 kbar, from solubility measurements on SiO<sub>2</sub>-buffering mineral assemblages. *Contributions to Mineralogy and Petrology* **146**, 135-143.
- Newton RC, Manning CE (2006). Solubilities of corundum, wollastonite and quartz in H<sub>2</sub>O-NaCl solutions at 800 degrees C and 10 kbar: Interaction of simple minerals with brines at high pressure and temperature: *Geochimica et Cosmochimica Acta*, **70**, 5571-5582.
- Nordstrom DK, Munoz JL, (1994) Geochemical thermodynamics. Blackwell Scientific Publications.
- Novgorodov P (1975). Quartz solubility in H<sub>2</sub>O-CO<sub>2</sub> mixtures at 700°C and pressures of 3 and 5 kbars. *Geokhimiya* **10**, 1484-1489.
- Pitzer KS (1973). Thermodynamics of electrolytes I. Theoretical basis and general equations. *Journal of Physical Chemistry* **77**, 268-277.
- Pitzer KS, Kim JJ (1974). Thermodynamics of electrolytes IV. Activity and osmotic coefficients for mixed electrolytes. *Journal of the American Chemical Society* **96**, 5701-5707.
- Powell R, Holland T, Worley B (1998). Calculating phase diagrams involving solid solutions via non- linear equations, with examples using THERMOCALC *Journal of Metamorphic Geology* **16**, 577-588.
- Renard F, Gratier JP, Jamtveit B (2000). Kinetics of crack-sealing, intergranular pressure solution, and compaction around active faults. *Journal of Structural Geology* **22**, 1395-1407.
- Sherman DM, Collings MD (2002). Ion association in concentrated NaCl brines from ambient to supercritical conditions: Results from classical molecular dynamics simulations. *Geochemical Transactions* **3**, 102-107.

- Shmulovich K, Graham C, Yardley B (2001). Quartz, albite and diopside solubilities in H<sub>2</sub>O-NaCl and H<sub>2</sub>O-CO<sub>2</sub> fluids at 0.5-0.9 GPa. *Contributions to Mineralogy and Petrology* **141**, 95-108.
- Shmulovich KI, Graham CM (1996). Melting of albite and dehydration of brucite in H<sub>2</sub>O-NaCl fluids to 9 kbars and 700-900 degrees C: Implications for partial melting and water activities during high pressure metamorphism: *Contributions to Mineralogy and Petrology* **124** 370-382.
- Shmulovich K, Graham C, Yardley B (2001). Quartz, albite and diopside solubilities in H<sub>2</sub>O-NaCl and H<sub>2</sub>O-CO<sub>2</sub> fluids at 0.5-0.9 GPa. *Contributions to Mineralogy and Petrology* **141**, 95-108.
- Shmulovich KI, Yardley BWD, Graham CM (2006). Solubility of quartz in crustal fluids: Experiments and general equations for salt solutions and H<sub>2</sub>O-CO<sub>2</sub> mixtures at 400-800 degrees C and 0.1-0.9 GPa. *Geofluids* **6**, 154-167.
- Somerfeld RA (1967). Quartz solution reaction: 400° - 500°C, 1000 bars. *Journal of Geophysical Research* **72**, 4253-4257.
- Stokes RH. (1991) Thermodynamics of solutions. In: *Activity coefficients in electrolyte solutions* (ed. K. S. Pitzer), pp. 1-28. Boston, U.S.A.,CRC Press.
- Thompson JBJ. (1982) Composition space: An algebraic and geometric approach. In: *Characterisation of metamorphism through mineral equilibria*, Vol. 10 (ed. J. M. Ferry), pp. 1-31. Washington, U.S.A.,Mineralogical Society of America.
- Walther JV, Orville PM (1983). The extraction quench technique for determination of the thermodynamic properties of solute complexes - application to quartz solubility in fluid mixtures. *American Mineralogist* **68**, 731-741.
- Wark DA, Watson EB (2002). Grain-scale channelization of pores due to gradients in temperature or composition of intergranular fluid or melt. *Journal of Geophysical Research-Solid Earth* **107**.

Xie ZX, Walther JV (1993). Wollastonite plus quartz solubility in supercritical NaCl aqueous-solutions. *American Journal of Science* **293**, 235-255.

Zotov N, Keppler H (2000). In-situ Raman spectra of dissolved silica species in aqueous fluids to 900°C and 14 kbar. *American Mineralogist* **85**, 600-604.

Zotov N, Keppler H (2002). Silica speciation in aqueous fluids at high pressures and high temperatures. *Chemical Geology* **184**, 71-82.

## Captions

### Figures

Figure 1. Types of quartz solubility behaviour, shown here for NaCl-bearing solutions. Type 1: Salt-out. Favoured by high density solutions with neutral and smaller ionic radii solutes. Type 2: Salt-in followed by salt-out. Enhanced by low density solutions and large ion lithophile solutes. S2006: Shmulovich *et al.* (2006). NM2000: Newton & Manning (2000).

Figure 2. Comparison between the error function approximation (solid lines) and ideal mixing formulations (broken lines) for  $\alpha$ , which records the extent of dissociation. The two formulations give similar but non-identical shapes. Success of the approximate formulation, in spite of the differences, is attributed to compensation for non-ideal behaviour and the existence of non-unique solutions to the quartz solubility equation.

Figure 3. Effects of model parameters on predicted Si solubility for a 1:1 electrolyte. (A)  $c$  is the ratio of the stability constants for alkali and silica species. High  $c$  gives more extreme salting in than low  $c$ . (B)  $d$  is the dissociation parameter. Increases in  $d$  reduce the degree of salting-in and decreases the apparent salt concentration for the silica concentration maximum. (C)  $n$  is the number of waters of hydration on the hydrated silica species. High  $n$  causes more extreme salting-out than low  $n$ . (D)  $b$  is the number of alkali molecules in the alkali-silica species. Low  $b$  causes more extreme salting-in than high  $b$  for any given ratio of the stability constants.

Figure 4. Results of model fits to NaCl-H<sub>2</sub>O data from the literature. (A) 0.1 GPa, 400 °C, Shmulovich *et al.* (2006); (B) 0.435 GPa, 600 °C, Newton & Manning (2000); (C) 0.9 GPa, 800°C, Shumulovich *et al.* (2001) and Shmulovich *et al.* (2006); (D) 1 GPa, 800 °C, Newton & Manning (2000). Model fits the data well across a wide range of temperature, pressure, and extremes of solubility behaviour.

Figure 5. Results of model fits to low pressure literature data. (A) 0.02 GPa, 350°C, NaCl, Fournier *et al.*(1982); (B) 0.03 GPa, 350°C, NaCl, Fournier *et al.* (1982); (C) 0.3

GPa, 600°C, KCl, Anderson & Burnham (1967); (D) 0.4 GPa, 600°C, KCl, Anderson & Burnham (1967). Model fits the data well across a wide range of temperature, pressure, and extremes of solubility behaviour.

Figure 6. Results of model fits to CsCl-H<sub>2</sub>O data from the literature. (A) 0.1 GPa, 400 °C, Shmulovich *et al.* (2006); (B) 0.2 GPa, 500 °C, Shmulovich *et al.* (2006); (C) 0.5 GPa, 800°C, Shmulovich *et al.* (2006); (D) 0.9 GPa, 800 °C, Shmulovich *et al.* (2006). Model fits the data well across a wide range of temperature, pressure, and extremes of solubility behaviour.

Figure 7. Initial results of model fits to CaCl<sub>2</sub>-H<sub>2</sub>O data from the literature. (A) 0.2 GPa, 800 °C, Shmulovich *et al.* (2006); (B) 0.5 GPa, 800 °C, Shmulovich *et al.* (2006); (C) 0.5 GPa, 500°C, Shmulovich *et al.* (2006); (D) 0.9 GPa, 500 °C, Shmulovich *et al.* (2006). Model fits the data well across a wide range of temperature, pressure, and extremes of solubility behaviour.

Figure 8. Interpolation of the calibration parameters: (A) measured  $c$  against predicted  $c$  for  $c$  fitted as a linear function of temperature and density. (B) measured  $d$  against predicted  $d$  for  $d$  fitted as a linear function of pressure and density. (C) quality of fit for data from Newton & Manning (2000) at 0.435 GPa and 700°C, using interpolated parameters. This data was not used in the fit. Figures in brackets are the fit calibration parameters and give some indication of the sensitivity of the model to the calibration parameters.; (D) quality of fit for data from Shmulovich *et al.* (2001) taken at 0.9 GPa and 800°C using interpolated fit parameters. The data shown was not used in the original fit.

Figure 9. Covariation of the model parameters. (A) dependence of  $\sigma$  the parameter that measures goodness of fit, on the set value of  $n$ , where  $n$  is the number of waters of hydration for the hydrated silica complex; (B) relationship between  $n$ , the number of waters of hydration for the hydrated silica complex, which is set by the modeller, and  $c$ , the fit parameter representing the relative stabilities of alkali and hydrated complexes; (C) relationship between  $n$ , the number of waters of hydration for the hydrated silica complex, which is set by the modeller, and  $d$ , the parameter that describes NaCl dissociation; (D)



relationship between  $c$ , the fit parameter representing the relative stabilities of alkali and hydrated complexes and  $d$ , the fit parameter that describes NaCl dissociation. The model parameters are not independent, and the solutions are not unique, but the parameters are not related in a simple way that would justify the use of an expression to reduce the number of parameters.

Figure 10. Comparison of  $\alpha_d$  and  $\alpha_K$  calculated for a  $d$  value of 2 with degree of dissociation calculated by THERMOCALC. The formulations agree at low apparent salt concentrations but diverge with increasing salinity.

Figure 11. (A) comparison between salting out induced by NaCl, CO<sub>2</sub> and CaCl<sub>2</sub> at 0.9 GPa and 500°C; (B) comparison between data for quartz solubility in CaCl<sub>2</sub>-bearing solutions with that predicted assuming different extents of dissociation of the CaCl<sub>2</sub>; (C) measured (points) and calculated (lines) quartz solubility in solutions where both dissociation of the CaCl<sub>2</sub> and reduction of water activity by ion solvation are considered. The observed data trends are consistent with moderate ion solvation.

## Tables

Table 1. Summary of data used in this paper. P: Pressure; T: Temperature; AB67: Anderson & Burnham (1967); F82: Fournier *et al.* (1982); NM2000: Newton & Manning (2000); S2001: Shmulovich *et al.* (2001); S2006: Shmulovich *et al.* (2006).  $n_{\text{meas}}$  is the number of measurements available. Solute concentrations are as apparent mole fractions.

Table 2. Summary of fits to data and results of interpolation for the datasets used in the interpolation exercise. P: Pressure; T: Temperature; \*: Indicates dataset used in the interpolation. †: there is a S2001 data point for these conditions but it is an outlier to the S2006 dataset and is therefore excluded. ‡: datasets with only three points, including the pure water system;  $\sigma_{\text{fit}}$  is not applicable for these datasets. AB67: Anderson & Burnham (1967); Fournier *et al.* (1982); NM2000: Newton & Manning (2000); S2001: Shmulovich *et al.* (2001); S2006: Shmulovich *et al.* (2006).

Table 3. Standard deviation between the fit and real  $c$  (Table 3a) and  $d$  (Table 3b) parameters when the parameters were assumed to be a linear function of the intensive parameters pressure, temperature, density, and dielectric constant.

## Tables

**Table 1**

Source	Solute	P(GPa)	T(°C)	X(solute) <sub>max</sub>	Type	n <sub>meas</sub>
AB67	KCl	0.4	700	0.167	2	9
AB67	KCl	0.3	600	0.166	2	6
AB67	HCl	0.3	600	0.11	2	4
AB67	KOH	0.3	600	0.001	3	3
FP82	NaCl	0.02	350	0.067	1	3
FP82	NaCl	0.03	350	0.067	1	5
FP82	NaCl	0.04	350	0.067	2	5
FP82	NaCl	0.05	350	0.067	2	4
NM2000	NaCl	0.2	700	0.516	1	5
NM2000	NaCl	0.435	600	0.368	2	3
NM2000	NaCl	0.435	700	0.502	2	6
NM2000	NaCl	0.435	750	0.594	2	3
NM2000	NaCl	1	500	0.22	2	4
NM2000	NaCl	1	600	0.33	2	3
NM2000	NaCl	1	700	0.44	2	4
NM2000	NaCl	1	800	0.58	2	15
NM2000	NaCl	1	850	0.653	2	5
NM2000	NaCl	1	900	0.76	2	5
NM2000	NaCl	1.5	700	0.365	2	4
S2001/S2006	NaCl	0.9	800	0.551	2	16
S2001	NaCl	0.9	650	0.221	2	4
S2001/S2006	NaCl	0.9	500	0.162	2	6
S2001/S2006	NaCl	0.5	800	0.398	2	13
S2006	NaCl	0.1	400	0.1923	1	4
S2006	NaCl	0.2	500	0.392	1	6
S2006	NaCl	0.5	500	0.242	2	10
S2006	NaCl	0.2	800	0.486	1	5
S2006	CaCl <sub>2</sub>	0.1	400	0.121	2	2
S2006	CaCl <sub>2</sub>	0.2	500	0.255	2	2
S2006	CaCl <sub>2</sub>	0.5	500	0.206	2	3
S2006	CaCl <sub>2</sub>	0.9	500	0.305	2	5
S2006	CaCl <sub>2</sub>	0.2	800	0.359	2	3
S2006	CaCl <sub>2</sub>	0.5	800	0.333	2	6
S2006	CaCl <sub>2</sub>	0.9	800	0.34	2	2
S2006	CsCl	0.1	400	0.287	1	4
S2006	CsCl	0.2	500	0.417	1	6
S2006	CsCl	0.5	500	0.408	1	8
S2006	CsCl	0.9	500	0.412	1	5
S2006	CsCl	0.2	800	0.531	1	8
S2006	CsCl	0.5	800	0.472	2	5
S2006	CsCl	0.9	800	0.469	2	3

**Table 2**

Source	Salt	P(GPa)	T (°C)	Fit	$n$	$b$	$c$	$d$	$\sigma_{\text{fit}}$	$\sigma_{\text{ex}}$
AB67	KCl	0.3	600	Aq + Alk	3	1.00	6.03	3.72	0.03	
AB67	KCl	0.4	700	Aq + Alk	3	1.00	147.07	121.82	0.04	
FP82	NaCl	0.05	350	Aq + Alk	3	1.00	6.45	15.08	0.01	
FP82	NaCl	0.04	350	Aq + Alk	3	1.00	7.00	11.61	0.02	
FP82	NaCl	0.03	350	Aq + Alk	3	1.00	10.16	12.27	0.01	
FP82	NaCl	0.02	350	Aq + Alk	3	1.00	13.03	9.86	0.03	
NM2000	NaCl	0.2	700	Aq + Alk	3	1.00	13.07	3.29	0.09	0.11*
NM2000 ‡	NaCl	0.435	600	Aq + Alk	3	1.00	4.83	4.47	0.00	0.10
NM2000	NaCl	0.435	700	Aq + Alk	3	1.00	4.57	3.95	0.02	0.10
NM2000 ‡	NaCl	0.435	750	Aq + Alk	3	1.00	3.54	2.88	0.00	0.07
NM2000	NaCl	1	500	Aq + Alk	3	1.00	0.50	1.36	0.03	0.06*
NM2000	NaCl	1	600	Aq + Alk	3	1.00	0.30	2.05	0.01	0.05*
NM2000	NaCl	1	700	Aq + Alk	3	1.00	0.33	2.33	0.03	0.03*
NM2000	NaCl	1	800	Aq + Alk	3	1.00	0.32	2.40	0.03	0.03*
NM2000	NaCl	1	850	Aq + Alk	3	1.00	0.32	2.80	0.02	0.04*
NM2000	NaCl	1	900	Aq + Alk	3	1.00	0.04	2.06	0.00	0.02*
NM2000	NaCl	1.5	700	Aq + Alk	3	1.00	0.19	1.38	0.01	0.28
S2001/S2006	NaCl	0.9	800	Aq + Alk	3	1.00	1.03	4.62	0.05	0.05
S2001	NaCl	0.9	650	Aq + Alk	3	1.00	0.50	88.11	0.06	0.07
S2001/S2006	NaCl	0.5	800	Aq + Alk	3	1.00	1.20	3.38	0.07	0.19*
S2006/S2006 †	NaCl	0.9	500	Aq + Alk	3	1.00	1.23	1.77	0.03	0.17
S2006	NaCl	0.1	400	Aq + Alk	3	1.00	12.27	5.13	0.04	0.06*
S2006	NaCl	0.2	500	Aq + Alk	3	1.00	6.78	3.31	0.05	0.07*
S2006	NaCl	0.5	500	Aq + Alk	3	1.00	4.96	24.16	0.02	0.11
S2006	NaCl	0.2	800	Aq + Alk	3	1.00	12.38	2.73	0.03	0.17*
S2006	CaCl <sub>2</sub>	0.5	800	Aq	6.27	n/a	n/a	n/a	0.03	
S2006	CaCl <sub>2</sub>	0.1	400	Aq	6.11	n/a	n/a	n/a	0.06	
S2006	CaCl <sub>2</sub>	0.2	500	Aq	4.98	n/a	n/a	n/a	0.05	
S2006	CaCl <sub>2</sub>	0.5	500	Aq	8.68	n/a	n/a	n/a	0.01	
S2006	CaCl <sub>2</sub>	0.9	500	Aq	9.42	n/a	n/a	n/a	0.06	
S2006	CaCl <sub>2</sub>	0.2	800	Aq + Alk	3	1.00	8.47	3.37	0.02	
S2006	CaCl <sub>2</sub>	0.9	800	Aq	5.87	n/a	n/a	n/a	0.02	
S2006	CsCl	0.1	400	Aq + Alk	3	1.00	15.91	2.48	0.02	
S2006	CsCl	0.2	500	Aq + Alk	3	1.00	11.07	2.42	0.03	
S2006	CsCl	0.5	500	Aq + Alk	3	1.00	5.94	2.47	0.02	
S2006	CsCl	0.9	500	Aq + Alk	3	1.00	6.43	2.51	0.08	
S2006	CsCl	0.2	800	Aq + Alk	3	1.00	15.26	2.32	0.11	
S2006	CsCl	0.5	800	Aq + Alk	3	1.00	3.31	2.37	0.05	
S2006	CsCl	0.9	800	Aq + Alk	3	1.00	1.58	2.18	0.00	

**Table 3a**

$\sigma_c$	P	T	$\rho$	$\varepsilon$
P	2.71	2.70	2.49	2.70
T	2.70	5.20	1.77	2.03
$\rho$	2.49	1.77	2.82	1.86
$\varepsilon$	2.70	2.03	1.86	4.72

**Table 3b**

$\sigma_d$	P	T	$\rho$	$\varepsilon$
P	0.60	0.60	0.56	0.60
T	0.60	0.97	0.71	0.65
$\rho$	0.56	0.71	0.82	0.77
$\varepsilon$	0.60	0.65	0.77	0.96

## Figures

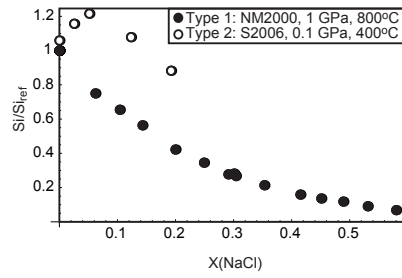


Figure 1:

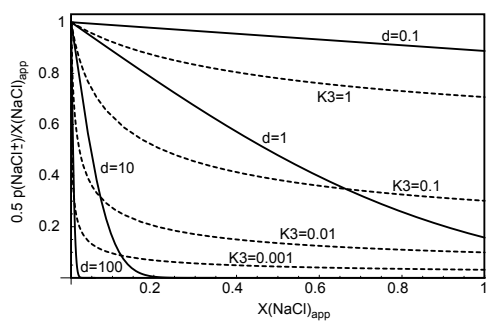


Figure 2:



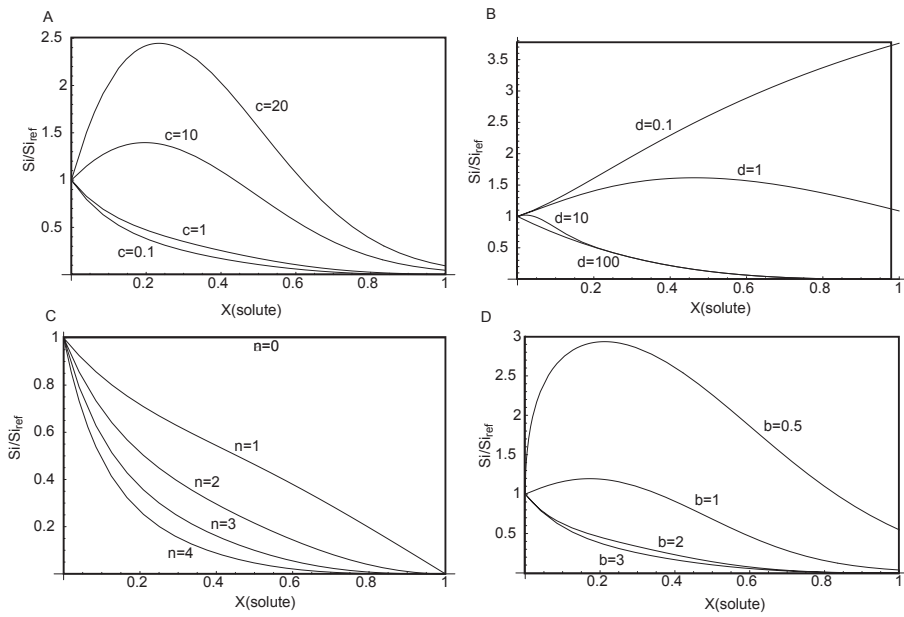


Figure 3:

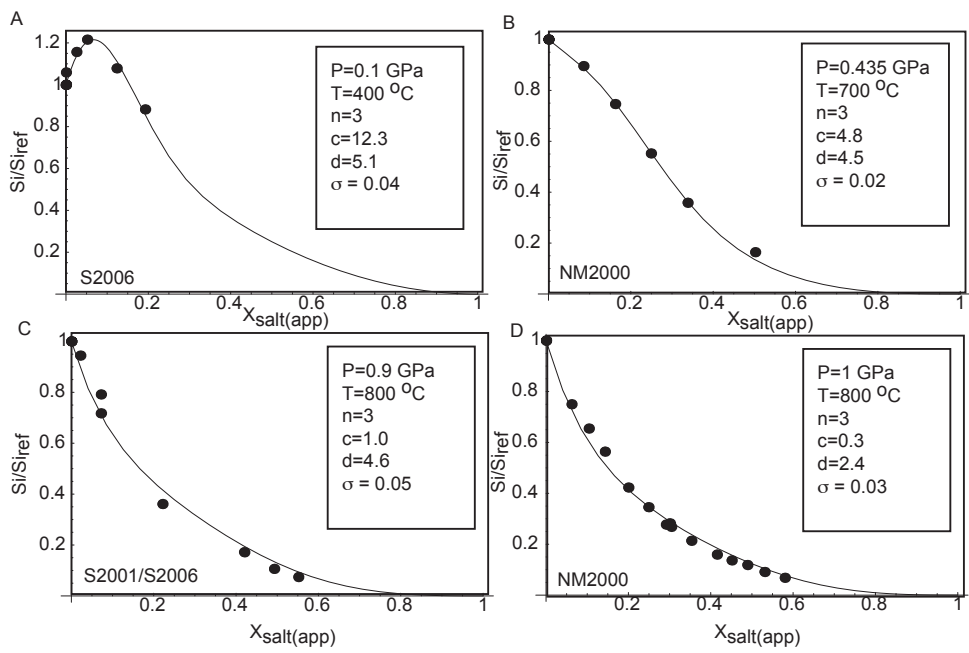


Figure 4:

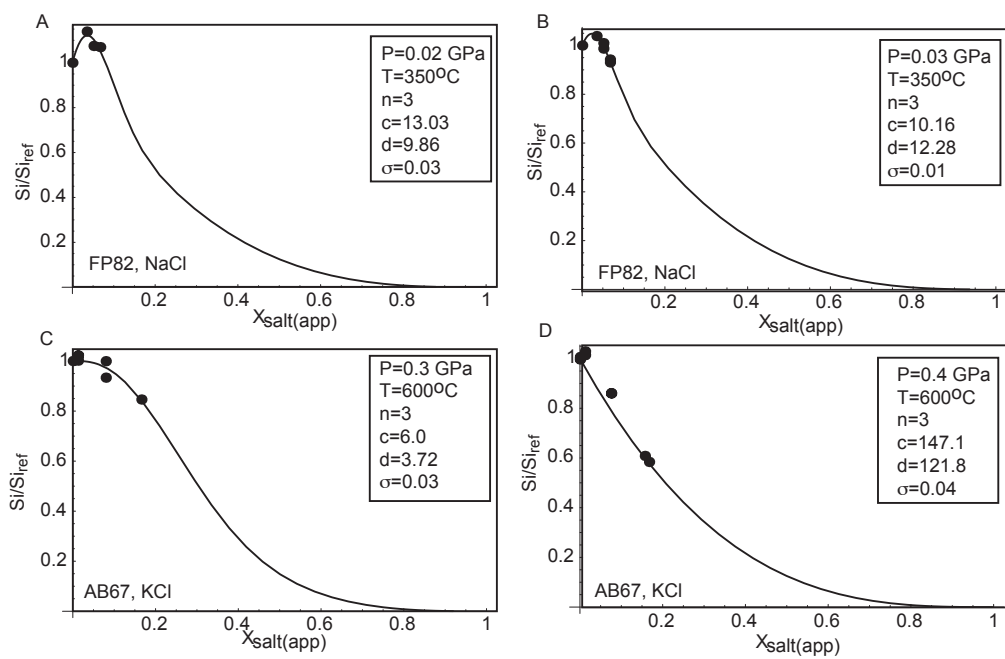


Figure 5:

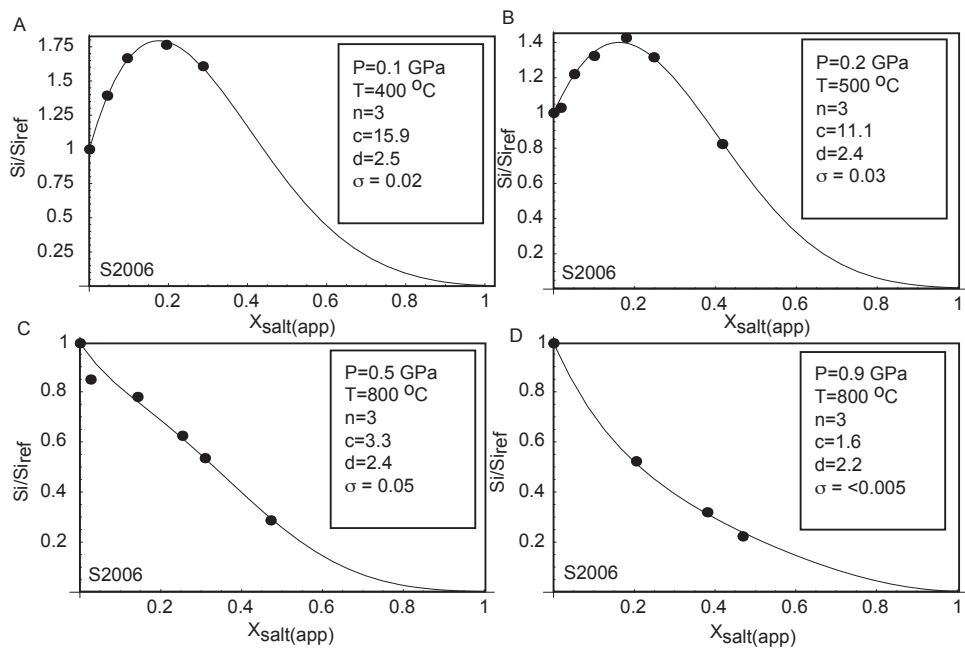


Figure 6:

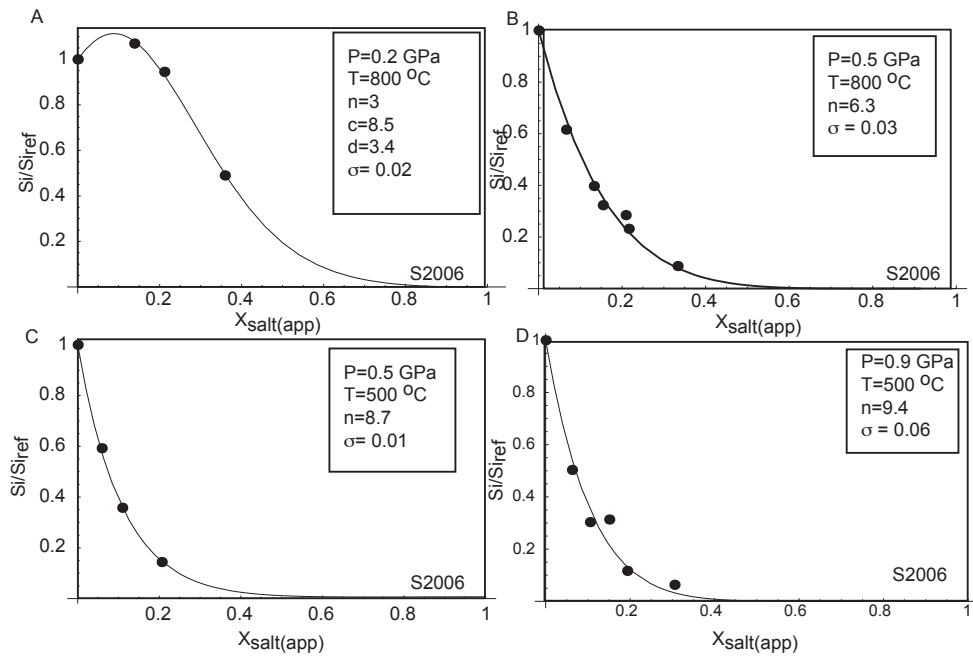


Figure 7:

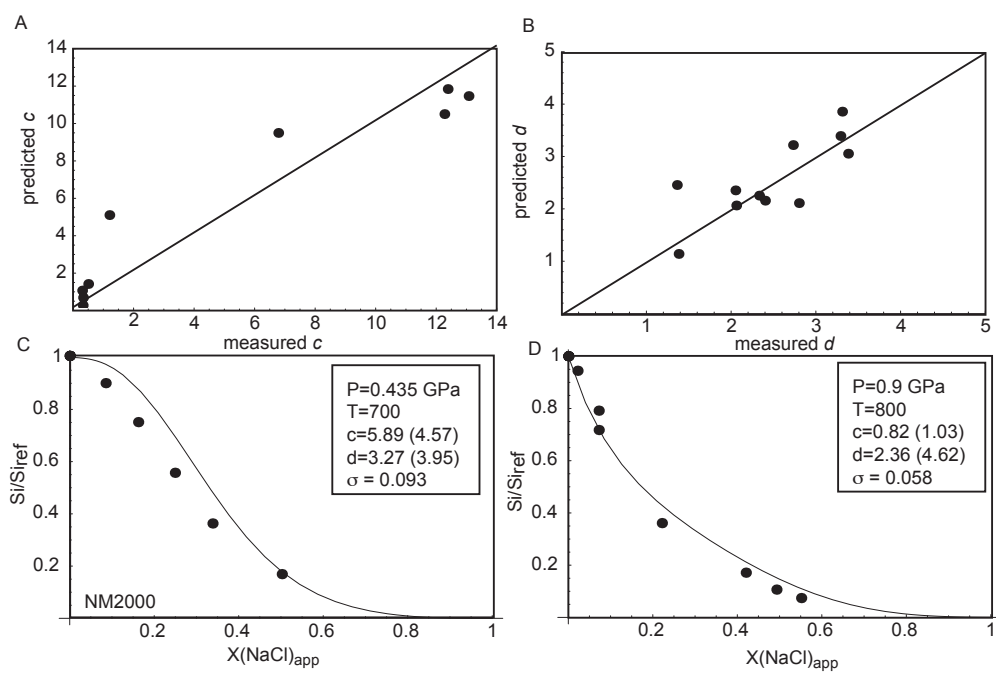


Figure 8:

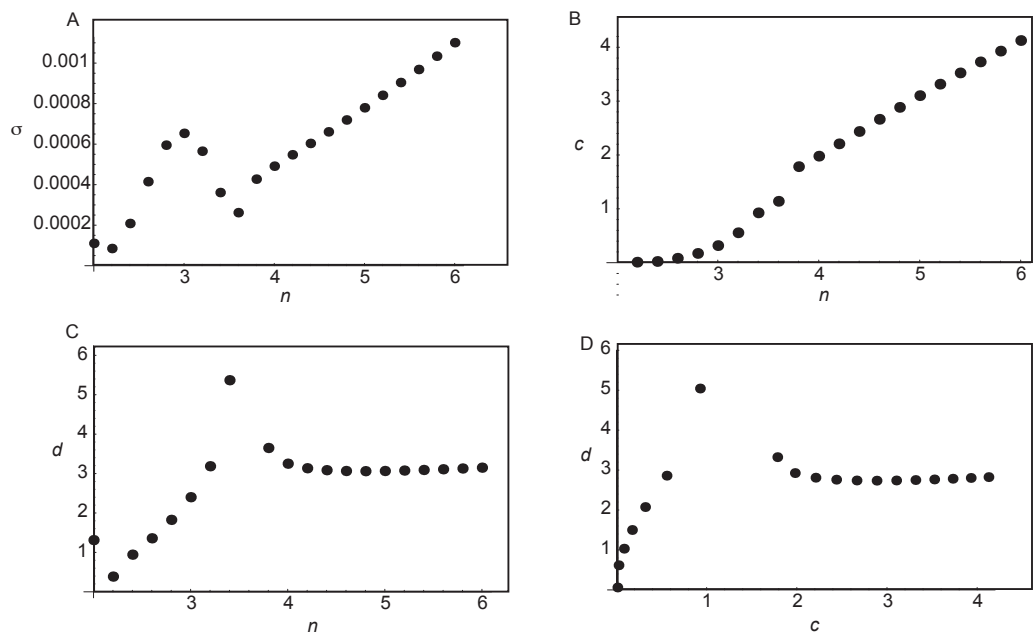


Figure 9:

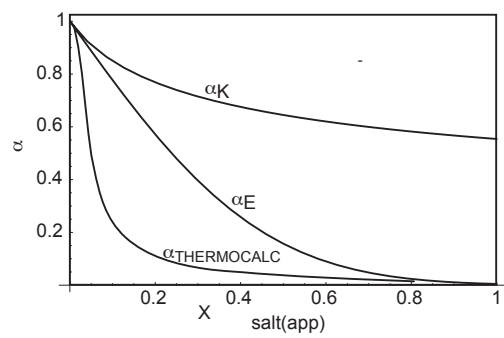


Figure 10:



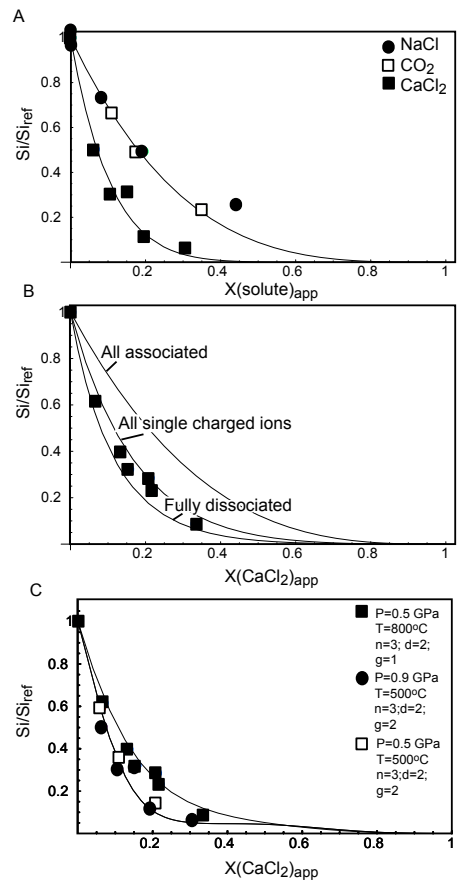


Figure 11: